

THERMAL EVOLUTION OF SUPERNOVA IRON IN ELLIPTICAL GALAXIES

Fabrizio Brighenti^{1,2} & William G. Mathews¹

¹*University of California Observatories/Lick Observatory, Department of Astronomy and Astrophysics, University of California, Santa Cruz, CA 95064*
mathews@ucolick.org

²*Dipartimento di Astronomia, Università di Bologna, via Ranzani 1, Bologna 40127, Italy*
brighenti@bo.astro.it

ABSTRACT

Interpretations of the spatial distribution, abundance ratios and global masses of metals in the hot gas of galaxy clusters in terms of supernova enrichment have been problematical. For example, the abundance of iron and other elements occasionally declines toward the center just where the stellar and supernova densities are highest. Also, the mass of gas-phase iron per unit stellar mass or light is lower in elliptical galaxies and groups than in rich galaxy clusters. We discuss hypothetical scenarios in which these abundance anomalies can result from the preferential buoyant separation of metals. However, in this and all previous attempts to explain these metallicity observations it has been assumed that all metals created by supernovae are present either in visible stars or the hot gas. We discuss here the possibility that some of the iron expelled into the hot gas by Type Ia supernovae may have radiatively cooled, avoiding detection by X-ray and optical observers. Hydrodynamic models of Type Ia explosions in the hot gas inside elliptical galaxies create a gas of nearly pure iron that is several times hotter than the local interstellar gas. We describe the subsequent thermal evolution of the iron-rich gas as it radiates and thermally mixes with the surrounding gas. There is a critical time by which the iron ions must mix into the ambient gas to avoid rapid radiative cooling. We find that successful mixing is possible if the iron ions diffuse with large mean free paths, as in an unmagnetized plasma. However, the Larmor radii of the iron ions are exceptionally small in microgauss fields, so the field geometry must be highly tangled or radial to allow the iron to mix by diffusion faster than it cools by radiative losses. The possibility that some of the supernova iron cools cannot be easily discounted.

Subject headings: cooling flows — diffusion — galaxies: elliptical and lenticular, CD — galaxies: ISM — X-rays: galaxies: clusters — supernova remnants

1. Introduction

We explore the possibility that some iron produced by Type Ia supernovae in galaxy groups and clusters may have radiatively cooled and avoided detection by X-ray and optical observers. Because of the large radiative emissivity of extremely iron-rich plasmas produced by Type Ia supernovae (SNIae), it is possible that this gas cools rapidly to low temperatures where it may be difficult to observe. Even if all SNIa iron radiatively cooled in an elliptical galaxy, the total collective X-ray luminosity would be small because the thermal energy content of the iron-rich cores in Type Ia supernova remnants is very much less than that of the radiating hot gas distributed throughout the galaxy or cluster.

Another motivation for this inquiry are the central abundance minima often observed in the hot gas inside central massive ellipticals in galaxy groups and clusters (Dupke & White, 2000; Johnstone, et al 2002; Sanders & Fabian 2002; Schmidt, Fabian & Sanders 2002; Blanton, Sarazin & McNamara 2003; Buote et al. 2003). When present, these minima typically lie within the central $\lesssim 30$ kpc, just where abundances in the hot gas are likely to be dominated by SNIae in the central elliptical galaxy. (The stellar density is more centrally peaked than the gas density.)

Another possible motivation is the observation of unexpectedly low iron abundance in the hot gas within some elliptical galaxies of moderate or low L_B . In a recent study of three X-ray faint elliptical galaxies O’Sullivan & Ponman (2004) found very low iron abundances in the interstellar gas, $z_{Fe} \lesssim 0.1z_{Fe\odot}$. Using *Chandra* data Humphrey, Buote & Canizares (2004) estimated $z_{Fe} \sim z_{Fe\odot}$ in the low L_x/L_B early-type galaxies NGC 1332 and NGC 720, perhaps indicating that \sim solar gas-phase iron abundances are more typical. However, the supersolar iron abundances predicted by our gasdynamical models for isolated elliptical galaxies typically exceed $z_{Fe\odot}$ (e.g. Mathews & Brighenti 2003).

Additional motivations for considering the cooling of iron-rich supernova remnants are (1) the difficulty of understanding how Type II and Type Ia supernovae enrich the hot gas in rich clusters of galaxies (Gibson & Matteucci 1997; Moretti et al. 2003; Baumgartner et al. 2003; Loewenstein 2004; Portinari et al. 2004; Tornatore et al. 2004, but see Tamura et al. 2004) and (2) the discord in metal abundances between rich galaxy clusters and galaxy groups or elliptical galaxies (e.g. Renzini 1997, 2000; Brighenti & Mathews 1999). Perhaps there are significant errors in supernova yields or in metallicity observations.

But in these recent attempts to understand the metal enrichment history of galaxy clusters, it is assumed that all of the iron produced by supernovae is still currently visible either in stars or in the hot gas. This is the assumption that we investigate here. It is necessary to establish that the iron visible today faithfully represents the total iron produced over time, particularly since the total historical number of supernovae in old stellar populations is uncertain. Alternatively, the lower iron content in groups and individual elliptical galaxies relative to massive clusters may be explained if supernova products are physically removed from the observed hot gas by winds or buoyancy. This scenario could simultaneously explain the relatively low iron abundance in gas associated with

individual non-cluster elliptical galaxies and the larger amount of gas-phase iron in clusters.

Morris & Fabian (2003) show that the enhanced radiative cooling of iron-rich inhomogeneities may occur without producing appreciable evidence of cooling in X-ray spectra. Unlike the iron-rich cooling discussed by Morris & Fabian – in which gas with different abundances was assumed to be at the same initial temperature – the iron in SNIa remnants is created at temperatures that significantly exceed that of the ambient hot gas, so the removal of SNIa iron by selective radiative cooling is not immediately obvious. In view of this we also estimate the inhomogeneity in SNIa iron that would be expected due to the sparse distribution of SNIa events on galactic scales.

In the following we describe possible thermal histories for the iron produced by SNIa explosions in elliptical galaxies. We begin with estimates of the post-supernova temperature of the iron-rich gas using gasdynamical models. This is followed by a discussion of possible scenarios for the rate that the iron-rich gas cools by thermal mixing and radiation losses. Our results suggest that much of the SNIa iron in cluster-centered elliptical galaxies may mix successfully with the ambient hot gas, but only if magnetic fields have little influence on the diffusion of iron ions.

2. Evolution of SNIa Remnants in Hot Gas

As we discuss below, the long term survival of iron introduced by Type Ia supernovae into the hot interstellar gas depends critically on the additional thermal energy imparted to the gas during the supernova explosion. Most calculations of the evolution of supernova remnants describe the early, luminous stages relevant to remnants observed in the Milky Way. Instead, we are interested in estimating the temperature of the iron-rich remnant gas after $10^4 - 10^5$ years when it has acquired essentially the same pressure as the local interstellar gas in a typical elliptical galaxy. The energy released by the β decay of cobalt, which sustains the SNIa light curve and decreases exponentially $\sim e^{-t/t_\beta}$ in $t_\beta \approx 100$ days, can be neglected in the total energy budget and on the very long time scales of interest here.

The one dimensional gas dynamical calculations of Mathews (1990) and Dorfi & Völk (1996) describe various aspects of Type Ia explosions in the rarefied gas in elliptical galaxies. The expanding stellar remnant cools by adiabatic expansion to exceedingly low temperatures and is then heated by a reverse shock as it is decelerated by the interstellar gas. From dimensional considerations, the characteristic temperature of the stellar iron is $T \sim (E_{sn}/M_{sn})m_p/k \sim 4 \times 10^9$ K for $E_{sn} = 10^{51}$ ergs and $M_{sn} = 1.4 M_\odot$. But this greatly overestimates the final iron temperature because (1) only a rather small amount of gas experiences shock velocities as large as $\sim (E_{sn}/M_{sn})^{1/2}$, and (2) only a comparatively small fraction of the supernova energy goes into heating the stellar gas in the stellar remnant – most of the supernova energy is delivered to the surrounding interstellar medium by an expanding shock wave.

To estimate the final temperature of the iron-rich gas we have calculated several simple one dimensional SNIa blast waves in the hot interstellar gas in elliptical galaxies. It is generally accepted

that small particle Larmor radii in microgauss magnetic fields allow these strong shocks to be treated with normal continuum gas dynamics and we assume this to be true. We also assume spherical symmetry which is unlikely to hold in detail. Non-spherical irregularities resulting from subsonic deflagration are expected inside the young stellar remnant and the deceleration of the expanding stellar gas results in Rayleigh-Taylor instabilities producing further spatial deformations. However, these details, which are ignored here, are unlikely to significantly influence our estimates of the mean gas temperature during the final stages of the remnant evolution when hydrostatic equilibrium is established throughout the iron-rich gas.

For an initial remnant configuration we employ the simple post-deflagration stellar remnant described for the W7 SNIa model of mass $M_{sn} = 1.4 M_{\odot}$ proposed by Dwarkadas & Chevalier (1998), which is based on the calculations by Höflich & Khokhlov (1996). The density distribution at time t_i is described by

$$\rho = \rho_o e^{-(r/r_s)} \quad \text{gm cm}^{-3}$$

with $r_s = v_s t_i$. The initial velocity field is linear $v = v_s r / r_s$. For any assumed initial time t_i integrations of $\rho(r)$ to a total mass $M_{sn} = 1.4 M_{\odot}$ and the kinetic energy density $\rho v_s^2 / 2$ to $E_{sn} = 10^{51}$ ergs determine ρ_o and the initial stellar radius r_s of the contact discontinuity between stellar and ambient gas. The initial time $t_i = 10^7$ sec for our calculations is chosen so that r_s is much less than the radius of ambient gas that contains the stellar mass ejected $r_m = (3M_{sn}/4\pi\rho)^{1/3} = 2.27/n_e^{1/3}$ pc where $\rho = 1.17n_e m_p$ and n_e are the ambient interstellar mass and electron densities.

To estimate the temperature of the iron plasma when the final SNIa remnant has reached pressure equilibrium, we calculated the evolution of several remnants for $\sim 10^5$ years using a high-resolution 1D Eulerian code. For simplicity the entire $1.4M_{\odot}$ star is assumed to be essentially pure iron ($z_{Fe} = 10^5 z_{Fe\odot}$); the hot ambient gas is assumed to have solar abundance. The code solves an additional equation for the iron density to determine the iron abundance $z_{Fe}(r, t)$. In Figure 1 we illustrate the gas temperature profile $T(r)$ after time $t = 5 \times 10^4$ years produced in interstellar medium of density $n_e = 0.01 \text{ cm}^{-3}$ and temperature $T = 10^7$ K. The vertical dashed line in Figure 1 shows the full extent of the stellar gas and the arrow points to the radius of the stellar core that includes $0.7 M_{\odot}$ of pure iron. The outer layers of the expanded star contain Si and other elements. At this time the stellar-interstellar contact discontinuity is at ~ 19 pc and the pressure is nearly uniform at all radii and equal to that in the initial ambient gas. Beyond the iron rich remnant the gas temperature decreases, reflecting the weakening of the expanding blast wave. The shock at $t = 5 \times 10^4$ yrs can be seen in Figure 1 as a small vertical feature at 65 pc. The temperature of the iron-rich stellar gas generally increases toward the center, corresponding to converging reverse shocks that grow stronger with time. An insignificant mass of gas near the center has a temperature comparable to $(E_{sn}/M_{sn})m_p/k$.

For the profile shown in Figure 1 we find that the mass weighted mean temperature in the central $0.7M_{\odot}$ is $\langle T \rangle_{0.7} \approx 6.7 \times 10^7$ K. Table 1 lists the mean gas temperatures $\langle T \rangle_{0.7}$ and $\langle T \rangle_{0.35}$ within the central 0.7 and $0.35M_{\odot}$ in the final pressure-equilibrium remnants (at time $t = 5 \times 10^4$ yr) computed for ambient gas at several densities and temperatures typical of hot gas at different

radii inside elliptical galaxies. All supernovae we consider have mass $M_{sn} = 1.4M_{\odot}$ and energy $E_{sn} = 10^{51}$ ergs. For interstellar gas at temperature 10^7 K, the final equilibrium iron plasma is heated by a factor of 6 or 7, but this factor decreases with increasing initial temperature of the ambient gas. In considering the subsequent thermal evolution of iron-rich gas in the following Section we consider $10^7 \lesssim \langle T \rangle \lesssim 3 \times 10^8$ K as representative of $\langle T \rangle$ values in Table 1. In the discussion below we describe how this gas cools by mixing with ambient interstellar gas at $T = 10^7$ K and by optically thin radiative emission.

3. Molecular Weight and Density

We consider a collisionally ionized plasma of hydrogen, helium and iron. The temperature range of interest extends from $T \sim 10^5$ K, where H and He are fully ionized, to $T \sim 3 \times 10^8$ K, corresponding to completely ionized iron (Sutherland & Dopita 1993). The molecular weight μ can be found from

$$\frac{1}{\mu} = \sum_j \frac{a_j}{A_j} n_{p,j} = 2a_H + \frac{3}{4}a_{He} + \frac{(1 + \bar{Z})}{A} a_{Fe}.$$

Here $n_{p,j}$ is the number of particles contributed by an atom of element j . The fraction of mass in element j is a_j and A_j is its atomic number, where $A \equiv A_{Fe} = 56$ for iron. Clearly $\sum a_j = 1$ and we adopt $a_{He}/a_H = 0.39$. Combining these results, the molecular weight is

$$\mu = \frac{1.39 + z_{Fe}}{2.29 + z_{Fe}(1 + \bar{Z})/A} \quad (1)$$

where $z_{Fe} = a_{Fe}/a_H$ is the abundance of iron relative to hydrogen by weight and $a_{Fe}/(a_H + a_{He}) = z_{Fe}/1.39$. For a pure iron plasma, the molecular weight is simply $\mu_{Fe} = A/(1 + \bar{Z})$.

If $x_{Fe,i}(T)$ is the fraction of iron ions with charge Z_i , the mean charge of iron ions

$$\bar{Z}(T) = \sum_i x_{Fe,i} Z_i \quad (2)$$

varies slowly with temperature in collisional equilibrium. In Figure 2 we plot $\bar{Z}(T)$ from Sutherland & Dopita (1993) together with a simple analytic fit

$$\begin{aligned} \bar{Z}(T) = & [2.074(1 - \phi) + 3.387\phi] \log T \\ & + [8.136(1 - \phi) - 13.12\phi] \end{aligned}$$

where

$$\phi = \{1 - \tanh[\log(T/10^{6.5} \text{ K})/0.55]\}/2.$$

For temperatures $10^5 \lesssim T \lesssim 10^8$ K, the energy radiated by line excitation and emission exceeds that in bremsstrahlung and other continua. In a plasma that cools by electron-ion collisions the

cooling rate depends critically on the number of free electrons per ion. At these temperatures only heavy ions such as iron have bound electrons. For our plasma of H, He and Fe, the number of free electrons per iron ion is

$$\frac{n_e}{n_{Fe}} = \frac{1.20 + z_{Fe}\bar{Z}/A}{z_{Fe}/A}. \quad (3)$$

In a normal plasma with solar abundances ($z_{Fe\odot} = 1.83 \times 10^{-3}$) the number of electrons per iron ion is $n_e/n_{Fe} \approx 1.20A/z_{Fe\odot} = 3.67 \times 10^4$. However, in a pure iron plasma ($z_{Fe} \rightarrow \infty$) this ratio $n_e/n_{Fe} = \bar{Z} \sim 21$ is very much reduced. Since there are $\sim 10^3$ fewer electrons per iron ion available to excite iron transitions, the radiation efficiency of a pure iron plasma is less than might have been imagined. The critical iron abundance at which the number of electrons from H plus He equals that from iron is

$$z_{Fe,crit} \approx 1.20A/\bar{Z} \approx 3.20 = 1750z_{Fe\odot}, \quad (4)$$

assuming $\bar{Z} \approx 21$.

The total density expressed in terms of number densities is

$$\rho = m_p(n_H + 4n_{He} + An_{Fe}) = n_H m_p [1.39 + z_{Fe}] \quad (5)$$

where m_p is the proton mass, $n_{He} = 0.0977n_H$ and

$$n_{Fe} = n_H z_{Fe}/A. \quad (6)$$

The electron density is

$$n_e = n_H + 2n_{He} + \bar{Z}n_{Fe} = n_H [1.20 + z_{Fe}\bar{Z}/A]. \quad (7)$$

4. Radiative Cooling Coefficient

In the optically thin limit, the cooling coefficient Λ is defined so that the plasma loses energy by radiation at a rate $n_e n_H \Lambda$ erg cm⁻³ s⁻¹. Using the XSPEC program and assuming very high iron abundances, we have extracted the cooling coefficient $\Lambda_{Fe}(T)$ for a pure iron plasma, defined so that $n_{Fe} n_e \Lambda_{Fe}(T)$ is the total power radiated per unit volume. We have also computed the cooling coefficient $\Lambda_{noFe}(T)$ for an iron-free plasma with solar abundances for all the other elements (as listed by Feldman 1992). These cooling coefficients can be combined to give the cooling rate for any iron abundance z_{Fe} ,

$$\Lambda(T, z_{Fe}) = \Lambda_{noFe}(T) + (z_{Fe}/A)\Lambda_{Fe}(T). \quad (8)$$

As we illustrate in Figure 3, in an iron-rich plasma the cooling coefficient $\Lambda(T, z_{Fe})$ can be many orders of magnitude greater than that for a plasma with solar abundance. However, the emission rate $n_e n_H \Lambda(T, z_{Fe})$ approaches a finite value as $z_{Fe} \rightarrow \infty$ that is only about ~ 280 times larger than the emissivity at solar abundance, provided the gas density is held constant. For $z_{Fe} \gtrsim 100z_{Fe,\odot}$ the peak emission is shifted toward higher temperatures. The cooling coefficients shown in Figure 3 are our analytic fits to the XSPEC results for $\Lambda_{noFe}(T)$ and $\Lambda_{Fe}(T)$.

5. Cooling of an Iron-Rich Plasma by Mixing and Radiation

After heating by the reverse shock, the temperature of the iron core in SNIa remnants is about 2-15 times greater than that in the surrounding hot interstellar gas (Table 1). We shall estimate the subsequent thermal evolution of this iron-rich gas as it cools by radiation losses and by mixing with the cooler interstellar gas. The mixing processes that occur when the iron plasma encounters the ambient (solar abundance) plasma are exceedingly complex. The Rayleigh-Taylor instability that accompanies the deceleration of the stellar remnant greatly increases the surface area between the iron and ambient plasmas. This mixing process is further assisted by irregularities in the exploding star and by interstellar turbulence expected from observations and general theoretical considerations. However, coarse grain mixing of the iron is insufficient for our purposes. Mixing must occur on an *atomic* level to influence the radiation losses. Once the surface area at the plasma interface has been enormously increased by coarse grain mixing, particle diffusion is essential to mix individual iron ions into the ambient gas and this diffusion depends on the strength and orientation of the local magnetic field. In view of the profound difficulty in estimating the ion mixing time due to diffusion, we shall simply assume that this mixing occurs on a timescale t_m that we regard as a parameter.

The iron-rich gas cools by two processes: (1) thermal mixing with cooler ambient solar abundance gas and (2) radiative losses. At any time we assume that a fraction f of the mass of colder ambient gas has physically mixed with the current iron-rich supernova core. Initially when $f = 0$ the gas is essentially pure iron; when the mass of mixed ambient gas is much greater than that of the SNIa remnant, $f \rightarrow 1$ and the iron abundance is nearly that of the ambient gas (with $z_{Fe\odot}$). We assume for simplicity that this mixing occurs on a timescale t_m so that the fraction of cold gas that has mixed at time t is given by

$$f = 1 - e^{-(t/t_m)}. \quad (9)$$

Initially at $t = 0$ when $f = 0$ we consider a hot plasma at temperature $T_h \approx \langle T \rangle_{0.7}$ that is sufficiently iron-rich, $z_{Fe,h} \gtrsim z_{Fe,crit}$, so that the electrons contributed by iron dominate. For a plasma of any composition, the ratio of iron mass to total mass is $z_{Fe}/(1.39 + z_{Fe})$ (Equation 3). Consequently, as the iron-rich gas mixes with ambient gas at temperature $T_c < T_h$, the instantaneous iron abundance $z_{Fe}(t)$ is found from

$$\frac{z_{Fe}}{1.39 + z_{Fe}} = (1 - f) \frac{z_{Fe,h}}{1.39 + z_{Fe,h}} + f \frac{z_{Fe\odot}}{1.39 + z_{Fe\odot}}. \quad (10)$$

The numerical solution for the thermal variation of the iron-rich plasma during a small time interval proceeds in two steps: first we determine the thermal change due to mixing alone then we compute the losses due to radiation during that same time interval. During the mixing step the specific thermal energy $\varepsilon = 3P/2\rho = 3kT/2\mu m_p$ varies as the relative mass f of cold gas mixes in. For a given time step $\delta t = t^{n+1} - t^n$ Equation (9) can be used to determine the change in the fraction of cold gas $\delta f = f(t^{n+1}) - f(t^n) \equiv f^{n+1} - f^n$. The decreased iron abundance $z_{Fe}^{n+1} = z_{Fe}(f^{n+1})$ is

found from Equation (10). The specific thermal energy varies according to

$$(1 - f^n + \delta f) \frac{T_m^{n+1}}{\mu^{n+1}} = (1 - f^n) \frac{T^n}{\mu^n} + \delta f \frac{T_c}{\mu_c} \quad (11)$$

where $\mu^n \equiv \mu(T^n, z_{Fe}(t^n))$ and $\mu_c \equiv \mu(T_c, z_{Fe\odot})$. This equation is solved for the intermediate, post-mixed temperature T_m^{n+1} .

We assume that the entire cooling process occurs at constant pressure P_o so

$$\begin{aligned} P_o &= \frac{kT_m^{n+1} \rho^{n+1}}{\mu^{n+1} m_p} \\ &= \frac{kT_m^{n+1} \rho^{n+1}}{m_p} \frac{[2.29 + z_{Fe}^{n+1}(1 + \bar{Z})/A]}{[1.39 + z_{Fe}^{n+1}]} \end{aligned} \quad (12)$$

can be used to determine the total density ρ^{n+1} at this stage of the calculation. Intermediate values for the number densities n_H , n_{Fe} and n_e are found from the expressions derived earlier. This completes the mixing step of the calculation.

Radiative cooling at constant pressure P_o can be regarded as a two-step process corresponding to the two terms on the right hand side of the thermal energy equation

$$\frac{d\varepsilon}{dt} = \frac{P}{\rho^2} \frac{d\rho}{dt} - \frac{n_e n_H \Lambda(T, z_{Fe})}{\rho}. \quad (13)$$

First we allow the gas to cool from T_m^{n+1} by radiative losses at constant density and z_{Fe}

$$\delta T = - \frac{T_m^{n+1}}{t_{cool}} \delta t \quad (14)$$

where T_m^{n+1} is the intermediate temperature found from Equation (11) and

$$t_{cool}(T, z_{Fe}) = \frac{3}{2} \frac{(kT)^2}{P_o \Lambda} \frac{[2.29 + z_{Fe}(1 + \bar{Z})/A]^2}{[1.20 + z_{Fe} \bar{Z}/A]} \quad (15)$$

is the instantaneous radiative cooling time. However, the temperature at t^{n+1} following the radiative energy loss, $T_r^{n+1} = T_m^{n+1} + \delta T$, corresponds to a pressure $P_r^{n+1} = kT_r^{n+1} \rho^{n+1} / \mu^{n+1} m_p$ that generally is less than the constant pressure P_o assumed. To correct this, we apply an adiabatic compression corresponding to the first term in the thermal energy equation above,

$$T^{n+1} = T_r^{n+1} (P_o / P_r^{n+1})^{2/5}. \quad (16)$$

This is the final temperature at time $t^{n+1} = t^n + \delta t$. To complete this computational cycle, the time-advanced densities ρ , n_H , n_e and n_{Fe} are determined again from the equation of state (12) consistent with constant P_o and the final temperature.

5.1. A Typical Cooling Evolution

In Figure 4 we show a typical constant-pressure cooling pattern for an iron-rich plasma using parameters for which cooling by diffusive mixing and radiation losses are comparable: $t_m = 10^7$ yrs, $P_o = 2 \times 10^{-11}$ dyn cm $^{-2}$, $z_{Fe,h}(t = 0) = 10^5 z_{Fe\odot}$, $z_{Fe,c} = z_{Fe\odot}$, $T_h = 10^8$ K and $T_c = 10^7$ K. The top panel shows the assumed variation of the fraction of cold gas $f(t)$ and the iron abundance $z_{Fe}(t)$, both of which vary with time as required by Equations (9) and (10). For the parameters chosen for Figure 4, the gas temperature $T(t)$ and the instantaneous cooling time $t_{cool}(t)$ evolve in a peculiar manner. As the elapsed time continues toward $t_m = 10^7$ yrs, both the temperature and the cooling time decrease as expected. But then t_{cool} suddenly shoots up by almost two orders of magnitude. At that time the gas temperature actually increases toward $T_c = 10^7$ K as gas at that temperature continues to mix in, overriding the general decline in temperature expected from radiation losses. Eventually, at time $\sim 100t_m$ the gas finally cools by radiation in a catastrophic fashion. The bottom panel in Figure 4 shows the corresponding evolution of several plasma densities. The proton and electron densities increase monotonically as gas with solar abundance mixes in. The density of iron ions n_{Fe} decreases as expected until the final catastrophic cooling when all densities increase without limit. During mixing, the electron to iron ion density ratio n_e/n_{Fe} increases by about ~ 1000 as expected from the preceding discussion. Finally, we note that the change in slope of the cooling time t_{cool} at $\log T = 7.4$ is caused by the slope change at this temperature in $\Lambda(T)$ (Figure 3).

In Figure 5 we plot the final cooling times (to $T = 10^5$ K) for four assumed initial temperatures for the iron-rich plasma T_h and four pressures P_o , corresponding to different radii in the hot gas atmospheres of luminous elliptical galaxies. For each calculation the initial iron abundance in the supernova ejecta is $z_{Fe,h} = 10^5 z_{Fe\odot} = 183$. The mixing times t_m are varied over a wide range, recognizing the uncertainty in this important parameter. For all calculations the ambient interstellar gas has temperature $T_c = 10^7$ K and abundance $z_{Fe,c} = z_{Fe\odot}$. The constant pressure cooling times of the (unmixed) interstellar gas are shown as horizontal dashed lines for each assumed pressure P_o .

As cold gas is mixed into the radiating iron-rich gas on progressively longer timescales t_m , the cooling times plotted in Figure 5 first increase, then sharply decrease, then increase again. Similar non-monotonic $t_{cool}(t_m)$ profiles occur if T_c or $z_{Fe,c}$ are changed. In the following we explain this counterintuitive behavior in more detail.

When $T_h = T_c$, as shown in the upper left panel of Figure 5, the mixing does not cool the iron-rich gas but only dilutes it with gas having solar abundance. As the dilution or mixing time t_m increases smoothly, the cooling time t_{cool} suddenly drops precipitously at a particular value of $t_m = t_{m,crit}$. When $t_m \ll t_{m,crit}$, the plasmas with different abundance tend to mix completely before radiative cooling occurs and t_{cool} is just the cooling time of the interstellar gas with solar abundance (dashed lines for each P_o). Eventually, when t_m just exceeds $t_{m,crit}$, the supernova gas cools rapidly when it still has an iron abundance much greater than solar. As can be seen in Figure

5, the transition in $t_{cool}(t_m)$ is very sharp indeed – the cooling time drops by ~ 1000 .

In the other three panels of Figure 5 we illustrate the cooling time variation $t_{cool}(t_m)$ for the iron rich supernova ejecta using more realistic initial temperatures $T_h > T_c = 10^7$ K. As t_m approaches $t_{m,crit}$ from below, the cooling time increases. This can be understood by examining the cooling evolution $T(t)$ in more detail. The temperature and cooling time minima (as in Figure 4) become more pronounced when $T_h > T_c$, but after this minimum the gas temperature returns to T_c and cools on a longer timescale. When $T_h > T_c$, the sharp decrease in the cooling time in Figure 5 at $t_{m,crit}$ is followed by progressively longer cooling times as t_m increases further.

To demonstrate further the curious non-monotonic relationship between the cooling and mixing times, we illustrate in Figure 6 the cooling evolution for four values of $t_m = 10^5, 10^7, 2 \times 10^7$ and 2×10^8 years. All four cooling calculations refer to pressure $P_o = 2 \times 10^{-11}$ dyn cm $^{-2}$ and $T_h = 10^8$ K (as in the lower left panel of Figure 5). In the central panel of Figure 6 it is seen that the cooling time increases, then sharply decreases, then increases again as t_m increases monotonically. From the upper panel of Figure 6, if $t_m = 10^5$ and 10^7 years, the gas mixes completely to interstellar values before radiatively cooling, and the well-mixed iron cools radiatively on a timescale similar to that of the interstellar gas (with $z_{Fe\odot}$). However, for $t_m = 2 \times 10^7$ or 2×10^8 years, the supernova enriched gas radiatively cools before it fully mixes with the ambient gas and the supernova ejecta is selectively cooled. The central panel of Figure 6 shows how early mixing can prolong the final cooling time to low temperatures. For these values of P_o and T_h , the most rapid cooling occurs for $t_m \approx 2 \times 10^7$ years when the iron-rich gas cools about 17 times faster than the ambient gas. The bottom panel of Figure 6 shows the variation of the instantaneous cooling time $t_{cool}(t)$ evaluated with Equation (15). If the gas mixes before it cools significantly by radiative losses, the cooling time passes through a minimum and rises sharply thereafter, greatly prolonging the final rapid cooling that eventually occurs.

The relationships between the cooling and mixing times shown in each panel of Figure 5 appear to have a self-similar variation with each pressure P_o . In Figure 7 the variations of t_{cool} with t_m in Figure 5 are plotted again with both times normalized with the cooling time of the ambient gas $t_{cool,c} = t_{cool}(T_c, P_o, z_{Fe\odot})$. In Figure 7 all curves in each panel of Figure 5 merge into a single curve valid for all pressures P_o , confirming the self-similarity.

The self-similarity in Figure 7 is surprising since the instantaneous cooling time expressed by Equation (15) depends on $z_{Fe}(t)$ which evolves differently in each cooling calculation with different P_o . However, as we illustrate in Figure 6, the gas either cools when completely mixed or it cools when $z_{Fe} \gtrsim 100z_{Fe,c}$ (where $z_{Fe,c} = z_{Fe\odot}$) – there are no intermediate cases. In either limit, as $z_{Fe} \rightarrow z_{Fe\odot}$ or $z_{Fe} \rightarrow \infty$, t_{cool} approaches a constant value independent of z_{Fe} , and this is the origin of the self-similarity in Figure 7.

The magnitude of the sharp transitions in t_{cool} at $t_{m,crit}$ in Figure 7 can be understood as the ratio of cooling times between the interstellar gas (T_c) and the iron rich ejecta (T_h). As $t_m/t_{cool,c}$

increases through the discontinuity, the cooling time of the gas drops by a factor

$$\frac{t_{cool}(T_h)}{t_{cool}(T_c)} \approx \left(\frac{T_h}{T_c}\right)^2 \left[\frac{\Lambda_{noFe}(T_c)}{\Lambda_{Fe}(T_h)} \frac{1.20}{(2.29)^2} \frac{(1 + \bar{Z})^2}{\bar{Z}} \right].$$

The quantity in square brackets is $\sim 10^{-3}$ when $T_h = T_c$, but increases approximately as $\sim T_h/T_c$ when $T_h > T_c$. For $T_h \gtrsim 3 \times 10^8$ K the cooling time of the iron-rich gas can exceed that of the ambient gas at $T_c = 10^7$ K if t_m is sufficiently long. In general the critical mixing time $t_{m,crit}$ is proportional to T_h/P_o .

6. Iron Diffusion in NGC 5044

The discussion above suggests that rather small variations of uncertain parameters – t_m , E_{sn} , T_h , etc. – determine whether iron produced in SNIa explosions in elliptical galaxies either cools much faster than the ambient gas or thermally mixes with it and cools on a much longer timescale. For typical mean post-shock temperatures of SNIa iron in Table 1, $T_h \approx 7 \times 10^7$ K, the radiative cooling time is about an order of magnitude less than that of the ambient gas $T_c \approx 10^7$ K provided the mixing time is larger than a critical value,

$$t_{m,crit} \approx 2.54 \times 10^7 \left(\frac{P_o}{10^{-11} \text{ dyn cm}^{-2}} \right)^{-1} \times \left(\frac{T_h}{7 \times 10^7 \text{ K}} \right) \text{ yrs} \quad (17)$$

where the coefficient is found from Figure 5. Guided by Figures 6 and 7, to avoid rapid radiative cooling, the iron-rich SNIa gas must mix in time $t_m < t_{m,crit}$ with enough interstellar gas to reduce the iron abundance to at least $z_{Fe,crit} \sim 100z_{Fe,\odot}$. The mass of interstellar gas that satisfies this condition is

$$M_{c,mix} = \frac{1.4M_{Fe,sn}}{100z_{Fe\odot}} = 5.3 \frac{(z_{Fe,crit}/z_{Fe\odot})}{100} M_\odot \quad (18)$$

where $M_{Fe,sn} = 0.7 M_\odot$ is the mass of iron in each SNIa remnant and 1.4 accounts for the mass in helium.

The question of interest is whether the iron-rich remnant can thermally mix with $M_{c,mix}$ of ambient gas in time $t_m < t_{m,crit}$. To avoid premature rapid radiative cooling of iron in SNIa remnants, the mixing must be totally complete on the *particle* level; mixing of small but finite fluid masses will not alter the radiative cooling rates. (Note that mixing on particle scales does not necessarily produce a spatially uniform final iron abundance on galactic scales.) Unfortunately, the complexity of the irregular morphology of the SNIa iron and uncertainties about the rate of physical diffusion preclude a rigorous calculation of the mixing time t_m . Nevertheless, it is easy to estimate the minimum mean free path λ_{diff} required for iron ions to mix with mass $M_{c,mix}$ in $t_m < t_{m,crit}$, and this can be compared with the plasma mean free path and Larmor radius. We make these

estimates using the well-known hot gas atmosphere in the luminous elliptical galaxy NGC 5044. Observations suggest that a large fraction, but possibly not all, of the SNIa iron produced in NGC 5044 may have indeed thermally mixed into the hot interstellar gas (Mathews et al. 2004). The gas temperature T_c , electron density n_{ec} , gas density ρ_c , and stellar density ρ_* in NGC 5044 are listed in Table 2 at four representative galactic radii. For comparison the effective radius of NGC 5044 is $R_e = 10.0$ kpc. Local values of the critical mixing time $t_{m,crit}$ are also listed at each radius.

We wish to estimate the diffusion of iron into the ambient hot gas containing mass $M_{c,mix}$ around the stellar remnant. For simplicity we ignore the outermost stellar layers containing Si and other elements and the complex geometrical disturbances caused by the Rayleigh-Taylor instability. We suppose instead that a spherical, pure-iron remnant of radius $r_* \approx 19$ pc and mass $M_{sn} = 1.4 M_\odot$ is in direct contact with ambient gas of abundance $z_{Fe\odot}$ when the diffusive mixing begins. It is seen from Figure 1 that the temperature in this outer region drops sharply with radius, $T(r_{pc}) \approx 1.35 \times 10^5 T_c r_{pc}^{-3.15}$ K for $r_* = 19 < r < 40$ pc where T_c is the initial gas temperature prior to the explosion. We assume that this radial dependence of the post-shock equilibrium temperature in Figure 1 can be scaled for other values of T_c . The gas density in this region is given by $\rho(r_{pc}) \approx 1.14 \times 10^{-29} n_{ec} (P/P_s) r_{pc}^{3.15}$ gm cm $^{-3}$ where $P_s = 2.65 \times 10^{-11}$ dy cm $^{-2}$ is a reference pressure. The radius r_{mix} containing the critical ambient mixing mass $M_{c,mix}$, shown in Table 2, can be found by integrating the mass outwards from the contact discontinuity r_* at the stellar-interstellar interface. The mass-weighted mean temperature \bar{T} and mean density \bar{n}_e in the shell $r_* < r < r_{mix}$ is found from a similar integration. Values of these quantities at each galactic radius are listed in Table 2.

The distance r_{diff} that iron ions diffuse in time $t_{m,crit}$ is $r_{diff} \sim (Dt_{m,crit})^{1/2}$ where the diffusion coefficient $D \sim \langle v_{Fe} \rangle \lambda_{diff}$ depends on the (Maxwellian) mean thermal velocity of iron ions $\langle v_{Fe} \rangle = (8k\bar{T}/\pi 56m_p)^{1/2}$ and λ_{diff} is their effective mean free path. The condition that iron ions diffuse a distance $r_{diff} \approx r_{mix} - r_*$ in the critical cooling time $t_{m,crit}$ can be used to determine the minimum iron mean free path, $\lambda_{diff} \approx (r_{mix} - r_*)^2 / \langle v_{Fe} \rangle t_{m,crit}$ to avoid radiative cooling. Values of $t_{m,crit}$ (calculated with $T_h = 7.5 \times 10^7$ K) and λ_{diff} are listed in Table 2 at each selected radius in NGC 5044.

The likelihood that the SNIa iron mixes in less than time $t_{m,crit}$ can be evaluated by comparing the effective mean free path for diffusion λ_{diff} with the field-free Spitzer plasma mean free path and the Larmor radius of the iron ions. The crosssection for Coulomb scattering of iron ions in an unmagnetized plasma is

$$\begin{aligned} \sigma_C &= 2\pi^{1/2} e^4 (kT)^{-2} Z_{Fe}^2 Z_H^2 \ln \Lambda \\ &\approx 1.74 \times 10^{-15} (T/10^7 \text{ K})^{-2} \text{ cm}^2, \end{aligned}$$

where we adopt $\ln \Lambda = 40$ (e.g. Chuzhoy & Loeb 2004). The iron ions are assumed to diffuse through protons, ignoring helium ions for simplicity, and for $z_{Fe} \sim 100 z_{Fe,\odot}$ $n_H \gg n_{Fe}$. The field-free plasma mean free path for the diffusing iron is then $\lambda_{spitz} = 1/\bar{n}_H \sigma_C = 0.024 (T/10^7 \text{ K})^2 (n_e/0.01 \text{ cm}^{-3})^{-1}$ pc, where $\bar{n}_H = \bar{n}_e (4 - 3\mu)/(2 + \mu)$ is the mean proton density in the diffusion shell. Comparing

λ_{spitz} listed in Table 2 with the smaller mean free path λ_{diff} required to avoid rapid iron-rich cooling, we conclude that λ_{spitz} is generally large enough to ensure that the SNIa iron mixes into the ambient gas in $t_m \lesssim t_{m,crit}$. Mixing is particularly likely within the central galaxy $r \lesssim R_e$. But mixing is only guaranteed if the iron diffusion is unaffected by the local magnetic field.

If magnetic fields are present, the ability of the SNIa iron to mix may be lessened if the Larmor radius $r_{L,Fe}$ is less than λ_{spitz} . Values of the Larmor radius of iron ions, $r_{L,Fe} = 56m_p \langle v_{Fe} \rangle c / \bar{Z} e B$, listed in Table 2 are evaluated with $\bar{Z} = 21$ and $B = 3 \times 10^{-6}$ gauss. Clearly $r_{L,Fe} \ll \lambda_{spitz}$. If the magnetic fields are coherent over scales much larger than $r_{L,Fe} \sim 10^9$ cm, the diffusive mixing of iron will be greatly reduced except along field lines. From Figure 1 we see that the temperature is higher and the gas density is lower in the diffusion shell $r_{mix} - r_*$ compared to T_c and ρ_c in the undisturbed, pre-explosion gas. The radial expansion that lowered the density may have stretched and oriented the magnetic field in a more radial direction, enhancing the diffusive mixing. Alternatively, if the magnetic field is highly tangled on a range of small scales, as in strong MHD turbulence, the effective plasma mean free path may not be much less than λ_{spitz} (Narayan & Medvedev 2001). MHD turbulence may be necessary for the efficient mixing of SNIa iron into the hot gas.

One possible argument against the selective cooling of iron-rich SNIa remnants is that there are no known elliptical galaxies with stellar iron abundances greater than $1-2Z_{Fe\odot}$. However, such high stellar iron abundances would not be expected in elliptical galaxies since the number of these stars and their contribution to the integrated spectrum would be very small. Even if all the super-iron-rich gas in SNIa remnants cooled, the total star formation rate in NGC 5044 would be only $M_{c,mix} \alpha_{sn} (M_{*t}/M_{sn}) \approx 0.04 M_\odot \text{ yr}^{-1}$. The total mass of these stars would be an unobservable fraction of the stellar mass of NGC 5044, $M_{*t} = 3.4 \times 10^{11} M_\odot$.

7. SNIa Iron Inhomogeneities

The iron deposited in the hot interstellar gas by SNIa explosions is inherently inhomogeneous. The amount of inhomogeneity can be estimated by comparing the mean distance between SNIa events after some characteristic time to the distance that iron has diffused during that time. The rate that SNIa supernova remnants occur in elliptical galaxies is $\alpha_{sn} \rho_* / M_{sn}$ SNIae $\text{cm}^{-3} \text{ s}^{-1}$ where ρ_* is the stellar density and

$$\alpha_{sn} = 3.17 \times 10^{-20} \text{ SNU} \frac{(M_{sn}/M_\odot)}{\Upsilon_B} \approx 1.01 \times 10^{-21} \text{ s}^{-1}.$$

$\text{SNU} = 0.16$ is the current E-galaxy supernova rate in units of SNIae per $10^{10} L_B$ in 100 years (Cappellaro et al. 1999), $M_{sn} = 1.4 M_\odot$ is the typical mass ejected and we adopt $\Upsilon_B = 7$ for the stellar mass to B-band light ratio. After time t the mean distance between the centers of SNIa remnants is

$$d_{sn} = \left(\frac{M_{sn}}{t \alpha_{sn} \rho_*} \right)^{1/3}.$$

The local stellar density $\rho_*(r)$ in NGC 5044 shown in Table 2 is estimated from a de Vaucouleurs profile with total stellar mass $M_{*t} = \Upsilon_B L_B = 3.4 \times 10^{11} M_\odot$ and effective radius $R_e = 10.0$ kpc.

In Table 2 we list values of d_{sn} based on $t = t_{cool}(r)$, the constant-pressure radiative cooling time for interstellar gas with $T = 10^7$ K and $z_{Fe} = z_{Fe\odot}$. The time t_{cool} is a conservative measure of the radial flow time in the local interstellar gas. This time must be compared with the time for iron ions to diffuse a distance d_{sn} at the Spitzer rate, $t_{diff} \approx d_{sn}^2 / \langle v_{Fe} \rangle \lambda_{spitz}$. Comparing these times listed in Table 2, we see that $t_{diff} \lesssim t_{cool}$ for $r \lesssim R_e$. But at $r \gtrsim R_e$, the iron may not diffuse fast enough to achieve uniform abundance in the hot gas. It is likely, however, that the iron can be mixed to d_{sn} more efficiently by turbulent diffusion in the hot gas than our estimate suggests.

It is interesting to explore how the iron emission depends on the degree of iron inhomogeneity. Consider for simplicity a fixed volume V containing a mass M of gas with uniform solar iron abundance. Then imagine that the iron occupies a decreasing fraction $f_z = V_{Fe}/V \leq 1$ of the volume but that the pressure, the density and the total iron mass remain constant. Provided $z_{Fe\odot} < z_{Fe} < z_{Fe,crit}$, the bolometric iron luminosity

$$L_{Fe} = n_{Fe} n_e \Lambda_{Fe}(T) V_{Fe}$$

remains constant with decreasing $f_z \sim z_{Fe\odot}/z_{Fe}$ because of the conservation of iron $n_{Fe} V_{Fe}$ and n_e and $\mu = 0.61$ are unchanged as long as most of the electrons come from H and He. The ratio of total energy radiated when the iron occupies a volume fraction f_z to the energy radiated by uniformly distributed iron is $E_{Fe}/E_{Fe,0} \sim L_{Fe} t_{cool} / L_{Fe,0} t_{cool,0}$ and decreases in pace with

$$\frac{t_{cool}}{t_{cool,0}} \sim \frac{\Lambda_{noFe}/\Lambda_{Fe} + z_{Fe\odot}/A}{\Lambda_{noFe}/\Lambda_{Fe} + z_{Fe}/A}.$$

As z_{Fe} approaches $z_{Fe,crit}$ the ratio $L_{Fe}/L_{Fe,0}$ decreases slightly and asymptotically reaches the value $1.39\bar{Z}/1.2A \sim 0.44$. The ratio of total energy radiated by the iron approaches

$$\frac{E_{Fe}}{E_{Fe,0}} \sim 0.62 \frac{L_{Fe}}{L_{Fe,0}} \left[\frac{\Lambda_{noFe}}{\Lambda_{Fe}} + \frac{z_{Fe\odot}}{A} \right] \frac{A^2}{\bar{Z}} \sim 0.02.$$

So far we have assumed that the iron-rich region is in buoyant equilibrium with the surrounding gas (i.e. it has the same density). If instead we assume that the iron-rich gas is in thermal equilibrium with the initial ambient gas, $L_{Fe}/L_{Fe,0}$ and $E_{Fe}/E_{Fe,0}$ behave as in the preceding case when $z_{Fe} < z_{Fe,crit}$, but when $z_{Fe} \geq z_{Fe,crit}$ $L_{Fe}/L_{Fe,0}$ increases to $2.29\bar{Z}/1.2(1 + \bar{Z}) \sim 1.8$ and

$$\frac{E_{Fe}}{E_{Fe,0}} \sim 0.23 \frac{L_{Fe}}{L_{Fe,0}} \left[\frac{\Lambda_{noFe}}{\Lambda_{Fe}} + \frac{z_{Fe\odot}}{A} \right] \frac{(1 + \bar{Z})^2}{\bar{Z}} \sim 0.0036.$$

Morris & Fabian (2003) discuss the radiative cooling of iron-rich regions (with $0 < z_{Fe} < z_{Fe,crit}$) that have the same initial temperature and pressure as the surrounding gas. In this case, small iron-rich regions with high z_{Fe} cool rapidly, but radiate a total thermal energy that is $\sim f_z = V_{Fe}/V$ times less than that of the surrounding plasma. When integrated over time, this type of selective transient cooling of iron-rich regions emits less iron emission than if the same mass of iron cooled in a gas with uniform abundance (Morris & Fabian 2003).

8. Conclusions

We have explored the possibility that some of the iron produced in SNIa explosions in elliptical galaxies may cool much faster than ambient gas having a normal hot gas abundance $\sim z_{Fe\odot}$. The temperature evolution of the iron-rich gas is governed by optically thin radiation loss and by diffusive mixing with the ambient interstellar gas. For simplicity we have ignored any differential radial motion of the SNIa remnants relative to the surrounding gas. We assume that a fraction by mass $f(t) = 1 - e^{-(t/t_m)}$ of hot interstellar or group gas physically mixes with the SNIa iron, regarding t_m as an unknown mixing time. Radiative cooling and mixing are assumed to occur at constant pressure.

Our main conclusion is:

(1) The question whether iron in SNIa remnants can successfully diffuse into the hot interstellar gas in X-ray luminous elliptical galaxies depends on the uncertain magnetic field strength and geometry. If there is no field, the iron is expected to mix without catastrophic radiative cooling. However, if the magnetic field reduces the plasma mean free path of the iron ions by more than ~ 30 relative to the field-free value, the iron is likely to cool with very few observational consequences.

This conclusion is supported by the following more detailed results:

(2) Iron cores of SNIa remnants that have reached hydrostatic equilibrium with ambient gas at $T_c \approx 10^7$ K in elliptical galaxies typically have mass-weighted temperatures $T_h \approx 7T_c$.

(3) Iron-rich plasmas with abundances $30z_{Fe\odot} \lesssim z_{Fe} \lesssim z_{Fe,crit}$ cool rapidly by optically thin (iron) radiation losses with emissivity $\epsilon_{Fe} \approx 1.20n_H^2(z_{Fe}/A)\Lambda_{Fe}(T)$ erg s⁻¹ cm⁻³ where $A = 56$ is the atomic weight of iron. The critical iron abundance $z_{Fe,crit} = 1.2A/\bar{Z} \approx 3.2 \sim 1750z_{Fe\odot}$ is the abundance at which iron contributes the same number of electrons as H plus He, both assumed to be fully ionized, evaluated with $\bar{Z} = 21$. When $z_{Fe} > z_{Fe,crit}$ the emissivity of the iron-rich gas asymptotically approaches a constant value ~ 280 times larger than the emissivity of solar abundance gas at the same density.

(4) If the time t_m required for the iron-rich SNIa core to diffusively mix with ambient interstellar gas at constant pressure P exceeds a critical value $t_{m,crit} \sim 2.5 \times 10^7 (P/(10^{-11} \text{ dy cm}^{-2}))(T_h/7 \times 10^7 \text{ K})$ yrs, the cooling time of the iron-rich gas is reduced by $\sim 10^{-3}(T_h/T_c)^2$, where T_h and T_c are the temperatures of the iron in a young supernova remnant and the hot ambient gas respectively. This mixing must occur among iron and hydrogen ions, not on small but finite mass scales.

(5) The minimum effective mean free path of diffusing iron ions λ_{diff} required to successfully mix the iron-rich SNIa remnant in time $t_m < t_{m,crit}$ is $\gtrsim 30$ times smaller than the plasma mean free path λ_{spitz} , supporting the possibility that the SNIa iron successfully mixes with the surrounding

gas. However, the Larmor radius of iron ions in microgauss fields is very much smaller, $r_{L,Fe} \sim 10^{-10} \lambda_{spitz}$. Effective mixing of SNIa iron into the surrounding gas may be possible only if the magnetic field is highly tangled on small scales as in strong MHD turbulence or is stretched in the radial direction.

(6) Even if all the iron produced by SNIae in elliptical galaxies formed into super-iron-rich stars, the number of these stars would be insignificant and unobservable.

(7) If the iron diffuses at or near the Spitzer rate, the SNIa iron in elliptical galaxies may be mildly inhomogeneous, especially for $r \gtrsim R_e$.

As we discussed in the Introduction, SNIae are thought to furnish $\sim 3/4$ of the iron in the hot gas of massive clusters. Most of the iron is thought to be produced at early times, as indicated by the approximately constant iron abundance in the hot gas of rich galaxy clusters out to redshift $z \sim 1.2$ (Tozzi et al. 2003). This implies a much higher SNIa rate at $z \gtrsim 1$ than at the present time. X-ray luminous groups like NGC 5044, that appear to be gravitationally closed systems, contain less than half the iron found in rich clusters (Buote, Brighenti & Mathews 2004). The origin of this discrepancy is not understood. If iron-poor groups like NGC 5044 experienced the same enrichment history as rich clusters, it follows that much of the iron in groups has been buoyantly transported to unobservably large radii. Group winds may occur, but not in luminous groups like NGC 5044 that are baryonically closed.

If the metals are preferentially expelled on smaller galactic scales, this separation may extend to group scales in a natural way. In support of this idea, we speculate that that galaxies soon after formation are surrounded by low density halos of iron-rich, high-entropy gas. These halos could be produced by SNII and SNIa-driven winds, by the energy of low level AGN activity in elliptical galaxies, as we have discussed in Mathews et al. (2004) and elsewhere, or possibly by the buoyancy of individual SNIa remnants, particularly in dwarf galaxies. Later, when these galaxies enter the virial radius of a group and confront the relatively denser gas in the group, their tenuous iron-rich halos would be stripped. As more gas accumulates in the group, these high-entropy halos may buoyantly flow toward larger radii (and entropy) in the group gas at some fraction of the sound speed. Galactic halo bubbles of this type moving at $\sim 200 \text{ km s}^{-1}$ (about half the group gas sound speed) may move out 300 kpc, beyond the outermost gas currently observable in NGC 5044 and other similar iron-poor groups (Buote et al. 2004) in only ~ 1.5 Gyrs. Even if these hypothetical iron-rich, high-entropy, low-density halo bubbles moved more slowly, they would be difficult to observe in the outer regions of groups because of their relatively small size and low X-ray emissivity. Finally, the iron-rich gas in these galaxy halo bubbles may radiatively cool in $\sim 10^9$ yrs and be removed from observation.

On smaller scales within group and cluster-centered elliptical galaxies, it is likely that the hot iron-rich gas within individual SNIa remnants is buoyantly transported several kpcs to larger radii. This may explain the central abundance minima observed in NGC 5044 and other similar groups

and clusters.

If buoyant transport of iron-rich galactic halos in groups are the explanation for their apparent iron deficiency, groups like NGC 5044 should be surrounded by (as yet undetected) halos of very tenuous hot gas with an unusually high iron abundance. Using the observational data for NGC 5044 from Buote et al. (2004), hot gas detected within $r < 370$ kpc has a low mean gas phase iron abundance, $\langle z_{Fe} \rangle_{in} \approx 0.21 z_{Fe\odot}$. This inner region of NGC 5044 contains a total mass of $12.6 \times 10^{11} M_{\odot}$ of hot gas. Buote et al. (2004) estimate that the total gas mass extrapolated to the virial radius $r_{vir} = 870$ kpc is $M_{b,tot} = 45.5 \times 10^{11} M_{\odot}$ and this is approximately consistent with the cosmic baryon ratio. If the overall total gas phase iron abundance in NGC 5044 is the same as that of rich clusters, $\langle z_{Fe} \rangle_{tot} \approx 0.4 z_{Fe\odot}$, the unobserved hot gas (of mass $\sim 32.9 \times 10^{11} M_{\odot}$) beyond 370 kpc associated with the virialized dark halo of NGC 5044 would need to have an average iron abundance of $\langle z_{Fe} \rangle_{out} \approx 0.5 z_{Fe\odot}$ whether or not this hot gas is gravitationally bound to NGC 5044. Much of this as yet unobserved hot gas probably has an even higher iron abundance since the most distant iron abundance observed at $r = 300$ kpc, $z_{Fe} \approx 0.15 z_{Fe\odot}$, is very low. If iron is radially segregated this way in groups that later merge to form clusters, then we would expect pronounced iron inhomogeneities in rich clusters on scales of $\sim 10^{12} M_{\odot}$.

If future more detailed gasdynamic models can explain the group-cluster iron discrepancy and the central iron abundance dips in a natural way, there may be no compelling reason to assume that SNIa iron is lost by radiative cooling, but at present this type of remnant cooling must remain a possibility.

Studies of the evolution of hot gas in elliptical galaxies at UC Santa Cruz are supported by NASA grants NAG 5-8409 & ATP02-0122-0079 and NSF grants AST-9802994 & AST-0098351 for which we are very grateful.

REFERENCES

- Baumgartner, W.H., Loewenstein, M., Horner, D.J., & Mushotzky, R.F., 2003, ApJ, submitted (astro-ph/0309166)
- Blanton, E. L., Sarazin, C. L. & McNamara, B. R., 2003, ApJ, 585, 227
- Brighenti, F., Mathews, W. G. 1999, ApJ, 515, 542
- Buote, D. A., Brighenti, F. & Mathews, W. G., 2004, ApJ, 607, L91
- Buote, D. A., Lewis, A. D., Brighenti, F. & Mathews, W. G. 2003, ApJ, 595, 151 (P10)
- Cappellaro, E., Evans, R. & Turatto, M. 1999, A&A, 351, 459
- Chuzhoy, L. & Loeb, A. 2004, MNRAS, 349, L13
- Dorfi, E. A. & Völk, H. J. 1996, A&A, 307, 715

- Dupke, R. A. & White, R. E., III, 2000, *ApJ*, 537, 123
- Dwarkadas, V. V. & Chevalier, R. A. 1998, *ApJ*, 497, 807
- Feldman U. 1992, *Phys. Scripta*, 46, 202
- Gibson, B. K. & Matteucci, F. 1997, *ApJ*, 475, 47
- Humphrey, P.J., Buote, D.A., & Canizares, C.R., 2004, *ApJ*, in press (astro-ph/0406302)
- Johnstone, R. M., Allen, S. W., Fabian, A. C. & Sanders, J. S., *MNRAS*, 336, 299
- Loewenstein, M. 2004, *Carnegie Observatories Astrophysics Series*, vol. 4, in *Origin and Evolution of the Elements*, eds A. McWilliam and M. Rauch (Cambridge: Cambridge Univ. Press), p. 425
- Mathews, W. G. 1990, *ApJ*, 354, 468
- Mathews, W. G., Chomiuk, L., Brighenti, F. & Buote, D. A., *ApJ*, 616, 745
- Mathews, W. G., Brighenti, F. & Buote, D. A. 2004, *ApJ*, 615, 662
- Mathews, W. G., Brighenti, F., Buote, D. A. & Lewis, A. D. 2003, *ApJ*, 595, 159
- Mathews, W. G. & Brighenti, F. 2003, *Ann. Rev. Astron. & Astroph.*, 41, 191
- Narayan, R. & Medvedev, M. V. 2001, *ApJ*, 562, L129
- Moretti, A., Portinari, L. & Chiosi, C., 2003, *A&A*, 408, 431
- Morris, R. G. & Fabian, A. C. 2003, *ApJ*, 538, 559
- O’Sullivan, E. & Ponman, T. J. 2004, 349, 535
- Portinari, L., Moretti, A., Chiosi, C. & Sommer-Larsen, J., 2004, *ApJ*, 604, 579
- Rasmussen, J., Ponman, T.J., 2004, *MNRAS*, 349, 722
- Renzini, A., 1997, *ApJ*, 488, 35
- Sanders, J. S. & Fabian, A. C., 2002, *MNRAS*, 331, 273
- Schmidt, R. W., Fabian, A. C. & Sanders, J. S., 2002, *MNRAS*, 337, 71
- Spergel, D. N., et al. 2003, *ApJS*, 148, 175
- Sutherland, R. S. & Dopita, M. A. 1993, *ApJS*, 88, 253
- Tamura, T. et al. 2004, *A&A* 420, 135
- Tornatore, L., Borgani, S., Matteucci, F., Recchi, S. & Tozzi, P., 2004, *MNRAS*, 349, L19
- Tozzi, P., Rosati, P., Ettori, S., Borgani, S., Mainieri, V., & Norman, C., 2003, *ApJ*, 593, 705

Table 1. MEAN SNIA IRON REMNANT TEMPERATURES^a

n_e (cm^{-3})	T (K)	$\langle T \rangle_{0.35}$ (K)	$\langle T \rangle_{0.70}$ (K)
0.01	1.0×10^7	8.1×10^7	6.7×10^7
0.03	1.0×10^7	7.8×10^7	6.6×10^7
0.003	1.0×10^7	7.7×10^7	6.6×10^7
0.001	4.0×10^6	7.0×10^7	5.8×10^7
0.001	1.0×10^8	1.9×10^8	1.6×10^8

^a $\langle T \rangle_{0.35}$ and $\langle T \rangle_{0.70}$ are the mean mass-weighted final temperatures of iron in SNIa remnants within 0.35 and 0.70 M_\odot respectively. Remnants explode into uniform gas with density n_e and temperature T . For all calculations $t_i = 1 \times 10^7$ s, $E_{sn} = 10^{51}$ ergs and $M_{sn} = 1.4 M_\odot$.

Table 2. IRON DIFFUSION IN NGC 5044

		1.00	3.16	10.00	31.6
r	(kpc)	1.00	3.16	10.00	31.6
T_c	(K)	7.22×10^6	7.86×10^6	8.98×10^6	1.32×10^7
n_{ec}	(cm^{-3})	8.47×10^{-2}	3.88×10^{-2}	1.48×10^{-2}	4.15×10^{-3}
ρ_c	(g cm^{-3})	1.64×10^{-25}	7.53×10^{-26}	2.86×10^{-26}	8.05×10^{-27}
P_c	(dy cm^{-2})	1.60×10^{-10}	8.00×10^{-11}	3.48×10^{-11}	1.44×10^{-11}
ρ_*	(g cm^{-3})	1.19×10^{-22}	1.06×10^{-23}	5.81×10^{-25}	1.69×10^{-26}
$t_{m,crit}$	(yrs)	1.70×10^6	3.40×10^6	7.82×10^6	1.89×10^7
r_{mix}	(pc)	19.9	22.3	28.4	39.9
\bar{T}	(K)	8.72×10^7	7.65×10^7	5.13×10^7	3.04×10^7
\bar{n}_e	(cm^{-3})	6.90×10^{-3}	3.93×10^{-3}	2.55×10^{-3}	1.78×10^{-3}
$\langle v_{Fe} \rangle$	(km s^{-1})	181	170	139	107
λ_{diff}	(pc)	0.00431	0.0222	0.0836	0.215
λ_{spitz}	(pc)	2.46	3.32	2.31	1.16
$r_{L,Fe}$	(pc)	5.43×10^{-10}	5.09×10^{-10}	4.17×10^{-10}	3.21×10^{-10}
t_{cool}	(yrs)	6.9×10^7	1.4×10^8	3.2×10^8	7.7×10^8
d_{sn}	(pc)	72	127	253	614
t_{diff}	(yrs)	1.12×10^7	2.77×10^7	1.95×10^8	2.96×10^9

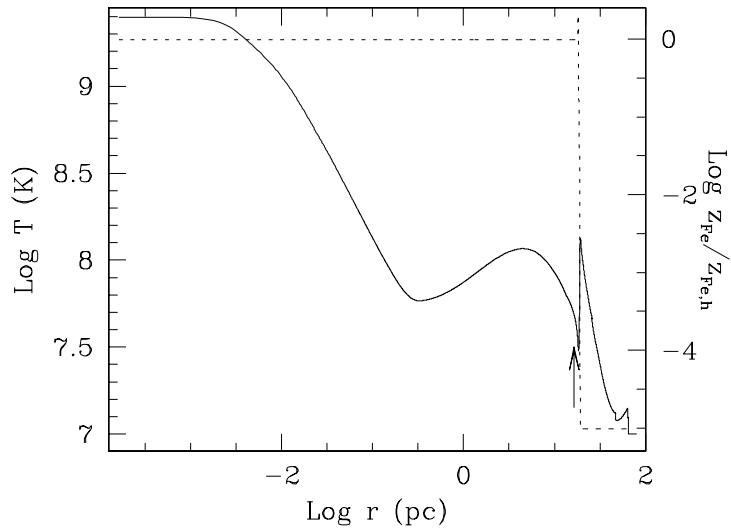


Fig. 1.— Temperature profile (*solid line*) of the stellar and ambient gas produced at time $t = 5 \times 10^4$ yrs by a SNIa supernova in hot gas of density $n_e = 0.01 \text{ cm}^{-3}$ and temperature $T = 10^7 \text{ K}$. The (*dashed*) line shows the computed iron abundance profile and the arrow points to the radius that contains $0.7 M_\odot$, the iron core of the SNIa remnant.

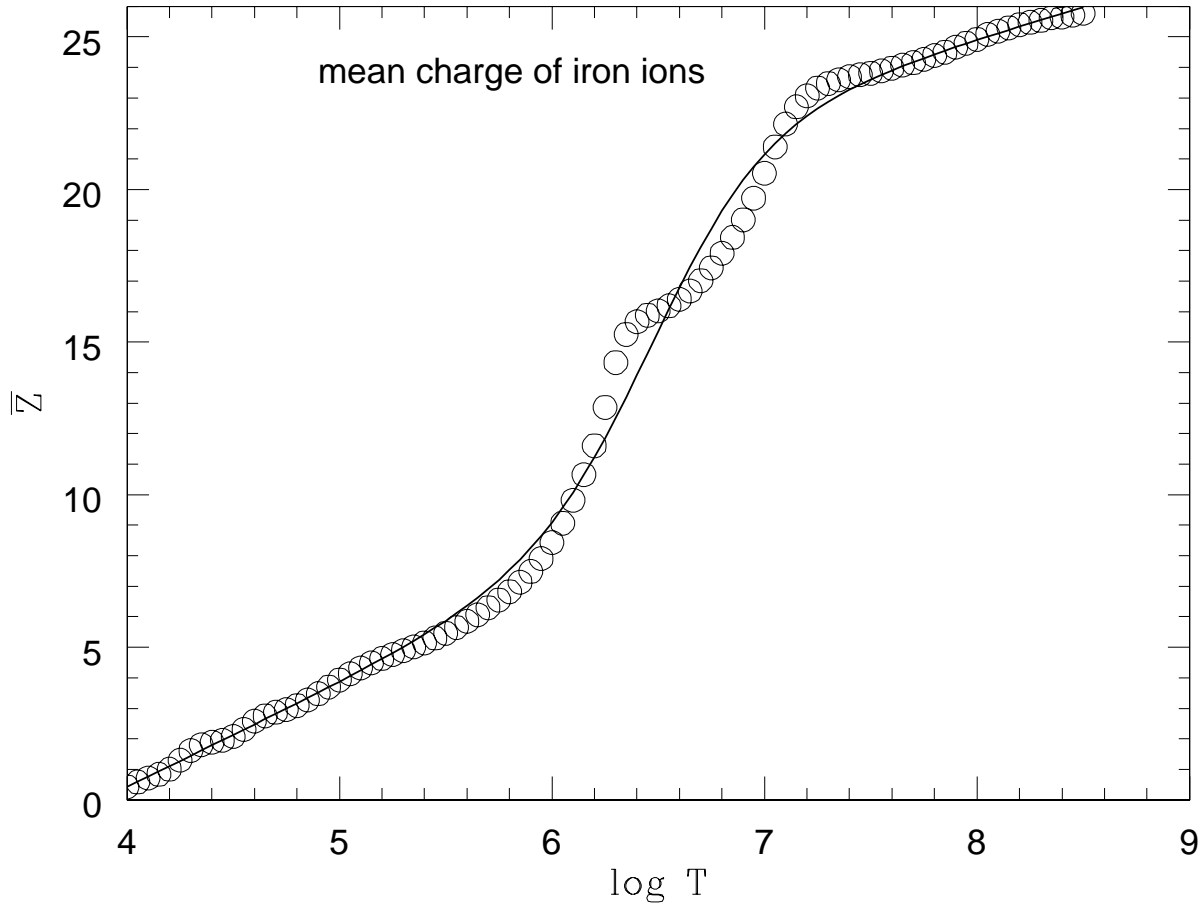


Fig. 2.— Mean charge of iron ions \bar{Z} in a collisionally ionized plasma (Sutherland & Dopita 1993) together with an approximate analytic fit.

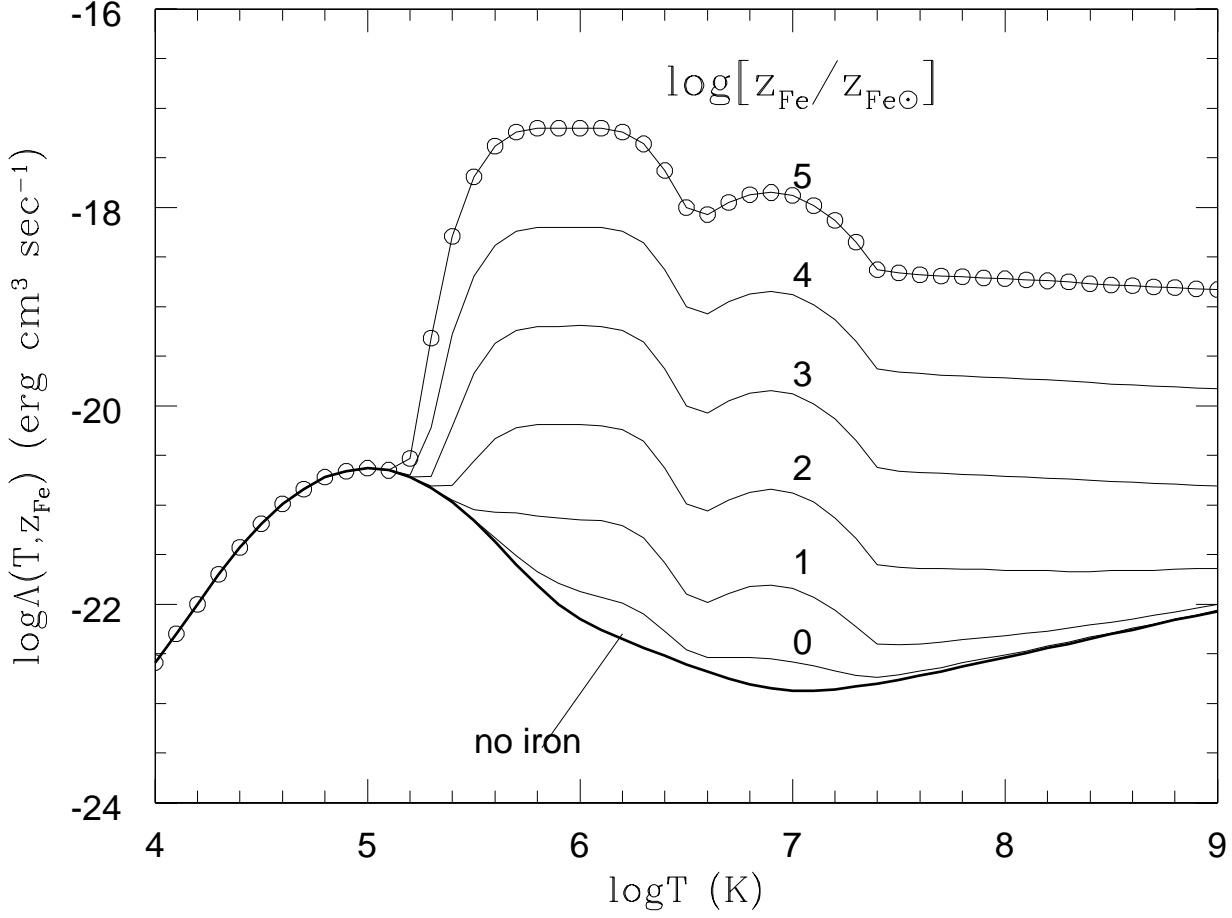


Fig. 3.— Comparison of radiative cooling coefficients without iron (*heavy curve*) and with increasing iron abundance. Each curve for $\log \Lambda(T, z_{\text{Fe}})$ is labeled with $\log[z_{\text{Fe}}/z_{\text{Fe}\odot}]$ where $z_{\text{Fe}\odot} = 1.83 \times 10^{-3}$. The light solid lines are fits to results computed with XSPEC. The open circles are the XSPEC results for $\log[z_{\text{Fe}}/z_{\text{Fe}\odot}] = 5$.

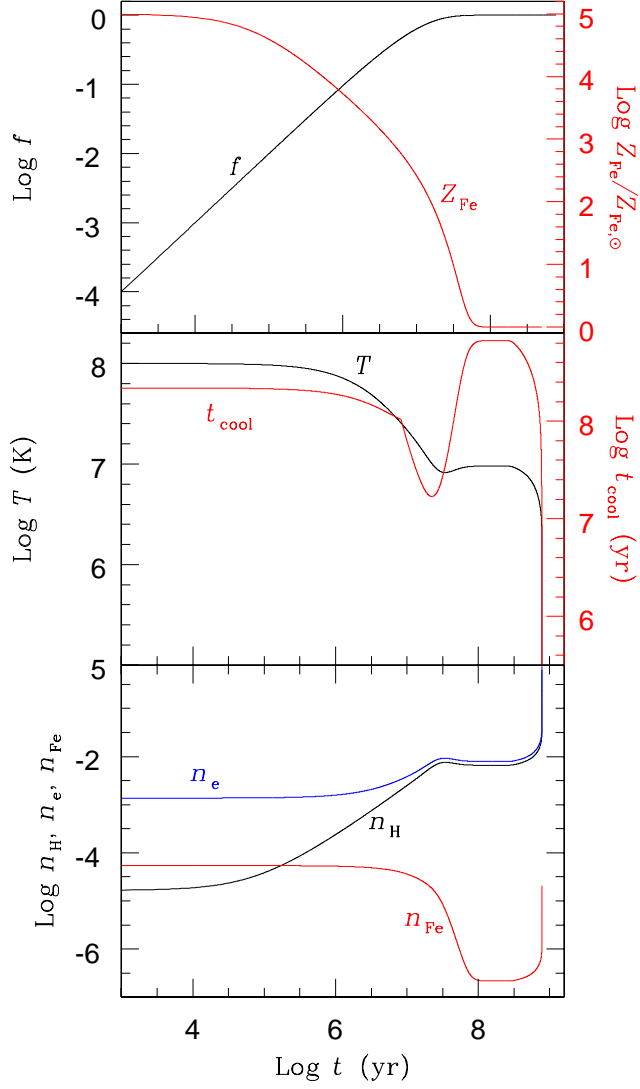


Fig. 4.— Thermal evolution of an iron-rich gas (initially with $z_{\text{Fe},h} = 10^5 z_{\text{Fe},\odot}$ and $T_h = 10^8$ K) mixing with an ambient gas (with $z_{\text{Fe},c} = z_{\text{Fe},\odot}$ and $T_c = 10^7$ K) at constant pressure $P_o = 2 \times 10^{-11}$ dyn cm $^{-2}$. The mixing time is $t_m = 10^7$ years. The upper panel shows the fraction $f(t)$ of mixed ambient gas and the abundance $z_{\text{Fe}}(t)$ of the mixture. The central panel shows the temperature $T(t)$ and the instantaneous cooling time. The bottom panel shows the number density of electrons, protons and iron ions.

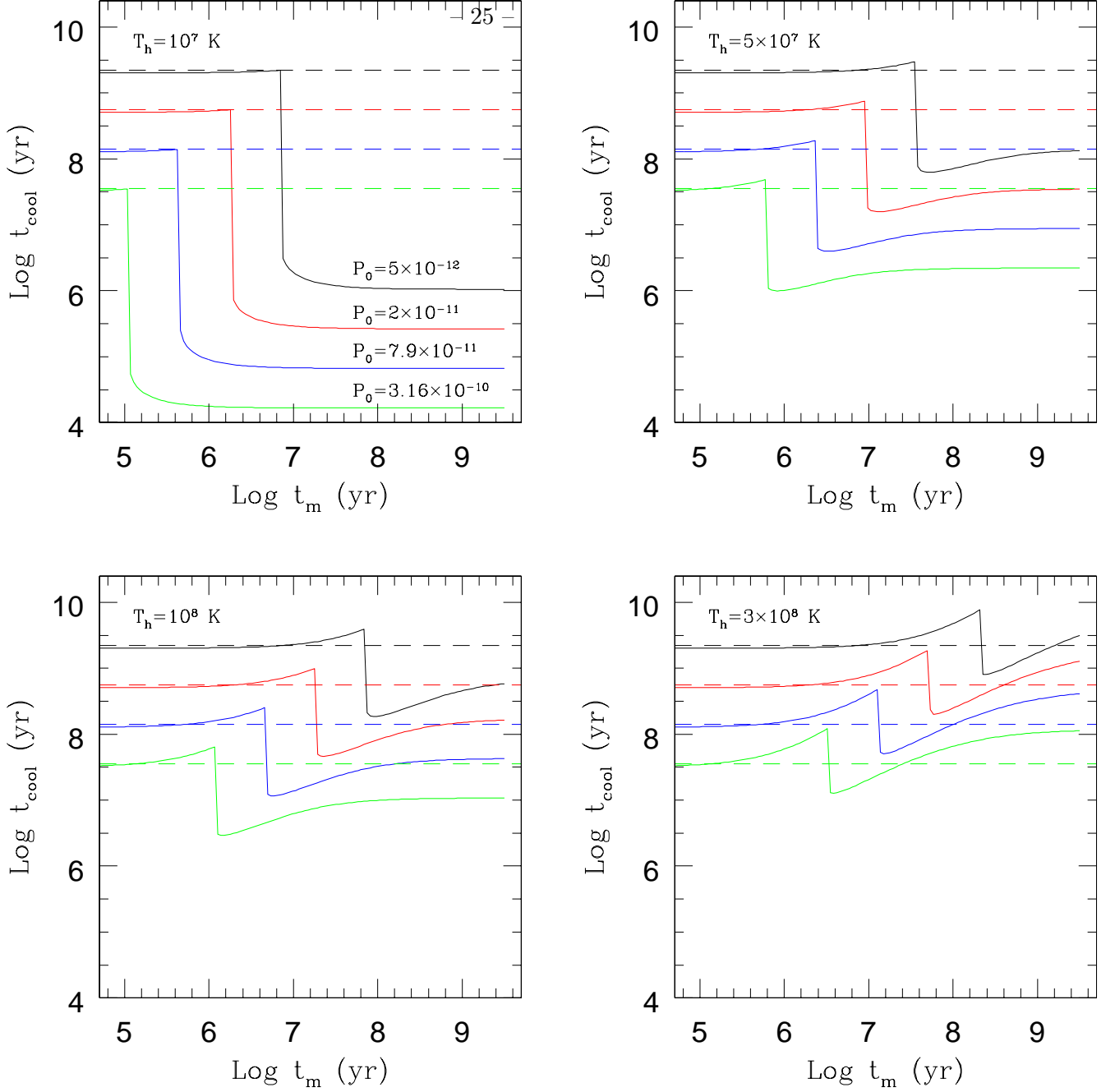


Fig. 5.— Variation of the cooling time (to $T = 10^5 \text{ K}$) as a function of the mixing time t_m with ambient gas at $T_c = 10^7 \text{ K}$. Each panel corresponds to a different initial temperature T_h for the hot iron-rich SNIa plasma (initially with $z_{Fe,h} = 10^5 z_{Fe\odot}$) and the four curves in each panel correspond to four pressures P_o (in dynes cm^{-2}) which remain constant during the cooling.

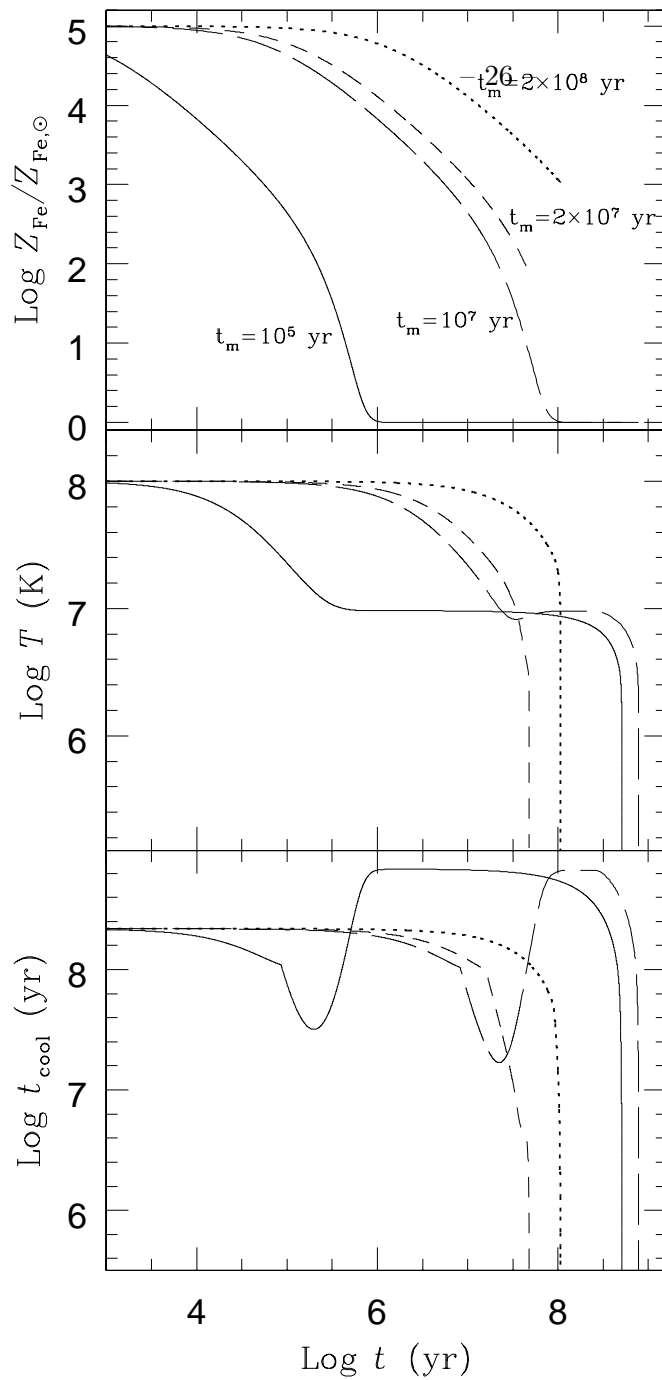


Fig. 6.— Time variation of four iron-rich cooling evolutions corresponding to four mixing times $t_m = 10^5$ yrs (solid lines), $t_m = 10^7$ yrs (long dashed lines), $t_m = 2 \times 10^7$ yrs (short dashed lines) and $t_m = 2 \times 10^8$ yrs (dotted lines). The curves show the iron abundance (top panel), the temperature (central panel) and the instantaneous cooling time (bottom panel).

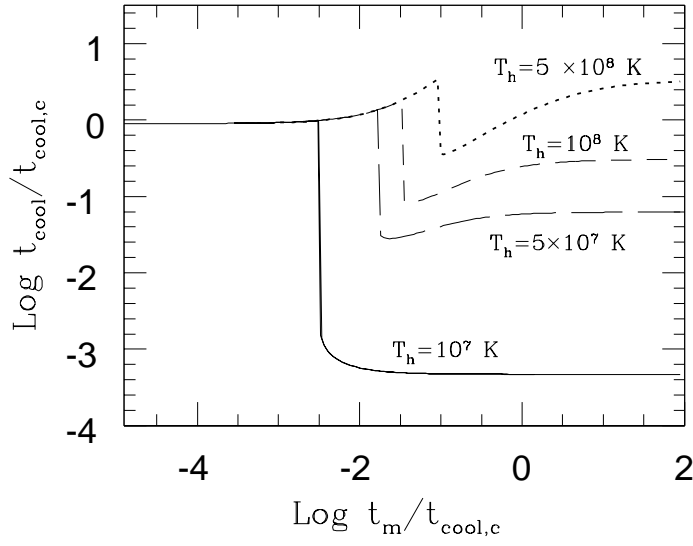


Fig. 7.— Variation of the cooling time (to $T = 10^5 \text{ K}$) as a function of the mixing time t_m with ambient gas at $T_c = 10^7 \text{ K}$ with both times normalized to the radiative cooling time of the ambient gas $t_{\text{cool},c}$. These curves are identical to those in Figure 5 and are valid for all pressures P_o .